Lymphoscintigraphy for interpretation of changes of cervical lymph node function in patients with oral malignant tumors: Comparison of Tc-99m-Re and Tc-99m-HSA-D

Tsuyoshi Sato, DDS, PhD,[a] Kohjirou Yamaguchi, DDS, PhD,[b] Yasuhiko Morita, DDS, PhD,[c] Takenori Noikura, DDS, PhD,[d] Kazumasa Sugihara, DDS, PhD,[e] and Shoji Matsune, MD, PhD,[f] Kagoshima, Japan
KAGOSHIMA UNIVERSITY DENTAL SCHOOL AND MEDICAL SCHOOL

Objective. The purpose of this study is to compare the usefulness of technetium-99m-rhenium colloid (Tc-99m-Re) and technetium-99m-human serum albumin diethylene-triamine-pentaacetic acid (Tc-99m-HSA-D) as lymphoscintigraphic agents and to discuss the significance of lymphoscintigraphy in comparison with computed tomography (CT), magnetic resonance imaging (MRI), and ultrasonography (US).
Study design. Dynamic and static lymphoscintigraphies were performed with Tc-99m-Re and Tc-99m-HSA-D. The usefulness of the 2 agents was evaluated statistically in comparison with pathologic findings and palpation. The significance of lymphoscintigraphy is discussed in comparison with CT, MRI, and US (by the literature of CT, MRI, and US).
Results. Lymphoscintigraphy was superior to palpation, and Tc-99m-Re was superior to Tc-99m-HSA-D in accuracy, specificity, and the incidence of true-positive and false-positive. Statistical significance was shown between the static lymphoscintigraphy with Tc-99m-Re and palpation. The reliability of lymphoscintigraphy seemed to be slightly inferior to CT and MRI in specificity and accuracy. However, lymphoscintigraphy had some advantages that CT and MRI lacked; for example, it showed very high sensitivity (100%) and no false-negative (0%). It also showed changes of lymph node function, showed all levels of neck nodes at one time, and showed a possibility of detecting small lymph node metastases.
Conclusion. Lymphoscintigraphy was more useful than palpation in detecting lymph node metastases, and Tc-99m-Re was superior to Tc-99m-HSA-D as an agent. Lymphoscintigraphy is significant when it is performed as a preliminary examination before CT or MRI. **(Oral Surg Oral Med Oral Pathol Oral Radiol Endod 2000;90:526-36)**

Early detection and complete control of lymph node metastases are the most important factors affecting the prognosis of malignant tumors.[1-3] Consequently, the regional lymph nodes are examined thoroughly by various imaging techniques. Computed tomography (CT), magnetic resonance imaging (MRI), and ultrasonography (US) are most often used for this purpose, and these methods provide useful information.[4-6] However, these methods display mainly morphologic changes in lymph nodes resulting from malignant tumors. On the other hand, lymphoscintigraphy offers a physiologic method for delineating the lymphatic drainages of regional lymph nodes and visualizes the changes in lymph node function.[7] In Japan, technetium-99m-rhenium colloid (Tc-99m-Re) and technetium-99m-human serum albumin diethylene-triamine-pentaacetic acid (Tc-99m-HSA-D) have been widely used for lymphoscintigraphy. Tc-99m-Re is a colloidal radioactive agent composed of small particles (2-15 nm).[8,9] The behavior of this radioactive agent strongly relates to its particle size.[10] First, Tc-99m-Re is taken into small lymphatic vessels when it is injected subcutaneously, and this uptake chiefly depends on the pore size of the vessels. Only particles of a specific size go through these small pores. Tc-99m-Re is composed of uniform particles of a suitable size for the pores and is easily taken. Next, Tc-99m-Re flows through small lymphatic vessels, then reaches lymph nodes, and finally is gormandized by lymph nodes. On the other hand, Tc-99m-HSA-D does not consist of any colloidal particles[11-13]; therefore, the mechanism of uptake of this radioactive agent in lymph nodes is very different from that of Tc-99m-Re. Generally, the dextran of a molecular weight over 40,000 is not taken into blood capillaries,[14] and substances of a molecular weight over 50,000 have a predisposition to be taken into small lymphatic vessels. The molecular weight of Tc-99m-HSA-D is over 50,000, so this agent easily moves into small lymphatic vessels and flows to lymph nodes when it is injected subcutaneously. However, Tc-99m-HSA-D is not gormandized by lymph nodes because it is not a colloidal radioactive agent and instead is just

[a]Associate Professor, Department of Dental Radiology.
[b]Associate, Department of Oral and Maxillofacial Surgery.
[c]Associate, Department of Dental Radiology.
[d]Professor, Department of Dental Radiology.
[e]Professor, Department of Oral and Maxillofacial Surgery.
[f]Lecturer, Department of Otorhinolaryngology.
Received for publication Nov 8, 1999; returned for revision Jan 30, 2000; accepted for publication Apr 10, 2000.

1079-2104/2000/$12.00 + 0 **7/16/109190**
doi:10.1067/moe.2000.109190

Table I. Case distribution

	Tc-99m-Re		*Tc-99m-HSA-D*	
Site of tumor	*Male*	*Female*	*Male*	*Female*
Maxilla	6	7	0	0
Mandible	4	1	1	0
Buccal mucosa	2	2	1	0
Tongue	12	6	7	1
Oral floor	16	2	3	1
Cervical region	7	0	6	0
Total	47	18	18	2
	(65)	85	(20)	

retained in lymph nodes.[11] Thus, Tc-99m-Re and Tc-99m-HSA-D differ in the mechanism of uptake, and because of this, their lymphoscintigraphic patterns are assumed to be different to some degree.

The criterion for metastatic lymph nodes in lymphoscintigraphy is based on the fact that normal lymph nodes can take Tc-99m-Re or Tc-99m-HSA-D, but metastatic lymph nodes either decrease uptake or cannot take it at all. In this study, we performed 2 types of lymphoscintigraphies, dynamic and static, and evaluated the various image patterns. We selected 3 image patterns on dynamic lymphoscintigraphy: asymmetric drainage, delayed drainage, and inverse drainage, and 5 image patterns on static lymphoscintigraphy: defect, mottled-patchy, swelling, collateral pathway, and rope-like finding, according to the criteria of Glassburn et al[15] and Kazem et al.[16] These image patterns on dynamic and static lymphoscintigraphies depend chiefly on the flow rate of radioactive agent in lymphatic vessels and the volume of the remaining normal lymph nodes and lymphatic vessels. Lymph node metastases usually cause changes of the flow rate in lymphatic vessels and changes of uptake of radioactive agent in lymph nodes. Therefore, the image patterns on dynamic lymphoscintigraphy mainly indicate the degree of obstruction of lymphatic vessels. In the image pattern on static lymphoscintigraphy, the defect locates the loss of normal lymph nodes, the mottled-patchy indicates the displacement of normal lymph node tissue by tumor in various degrees, the swelling shows the reactive hyperplasia of lymph nodes, the collateral pathway shows the new formation of lymphatic vessels, and the rope-like finding expresses the retention of radioactive agent caused by the obstruction of lymphatic drainage or dilatation of lymphatic vessels. Thus, lymphoscintigraphic image patterns can show the changes of lymph node function on the basis of the pathologic findings, and these images are useful as the criteria for evaluation of lymph node metastases.

Both Tc-99m-Re and Tc-99m-HSA-D have been used in lymphoscintigraphy of internal jugular chains for a long time, but there are few clinical reports on the differences between these 2 agents. In this report, the changes in internal jugular nodes caused by metastases from malignant tumors of oral and maxillofacial regions were prospectively examined by lymphoscintigraphy. The results from lymphoscintigraphy were correlated with those from the pathologic examination and palpation, and the usefulness of the 2 radioactive agents was compared. Furthermore, the significance of lymphoscintigraphy is discussed in comparison with CT, MRI, and US, which are now common techniques for detecting lymph node metastases.

MATERIALS AND METHODS

Patients

Lymphoscintigraphy with Tc-99m-Re was performed on 65 patients with squamous cell carcinomas of the maxilla (13 cases), mandible (5 cases), buccal mucosa (4 cases), tongue (18 cases), oral floor (18 cases), and cervical region (7 cases). The tumors of these 65 patients were classified according to T-staging: 21 cases of T1, 27 cases of T2, 15 cases of T3, and 2 cases of T4. Lymphoscintigraphy with Tc-99m-HSA-D was performed in 20 patients with squamous cell carcinomas of the mandible (1 case), buccal mucosa (1 case), tongue (8 cases), oral floor (4 cases), and cervical region (6 cases). These 20 consisted of 6 cases of T1, 12 cases of T2, and 2 cases of T3 (Table I). Patients who had undergone radiation therapy, surgical excision of primary tumors along with neck dissection before lympho-scintigraphy, or both were excluded from the study. Lymphoscintigraphy was performed as a part of the treatment-planning procedure for surgical treatment, including neck dissection.

Lymphoscintigraphy

The areas behind both ears were selected for the injection for lymphoscintigraphy. Either 0.25 mL of Tc-99m-Re (37 MBq) or 0.1 mL of Tc-99m-HSA-D (74 MBq) was injected subcutaneously into both postauricular areas. Images were obtained by using a Gamma View scintillation camera (Hitachi Co, Tokyo, Japan) with a low-energy ultra-high–resolution parallel hole collimator. Two types of imaging studies were performed, dynamic and static lymphoscintigraphy.

Dynamic lymphoscintigraphy was carried out immediately after the injection of the radioactive agent. The patient was placed on a bed in a prone position over the scintillation camera. Tc-99m-Re or Tc-99m-HSA-D was administered subcutaneously in both areas behind the ears by 2 dentists simultaneously. Scintiscans, each lasting 20 seconds, were obtained continuously for a period of up to 20 minutes. A 20-second scintiscan was recorded as a frame datum, and 60 frames were obtained. On each frame, 6 regions of interest (ROIs) covering both sides of the internal jugular chains were

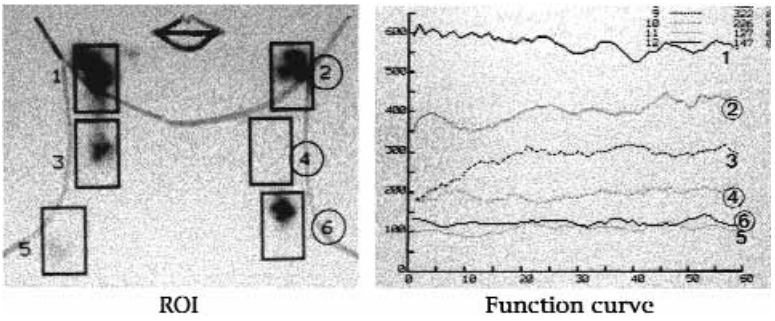

Fig 1. On each of 60 frame images, 6 ROIs cover both sides of internal jugular chains. ROI numbers 1, 3, and 5 cover right superior, mid, and inferior jugular nodes, and ROI numbers 2, 4, and 6 cover left superior, mid, and inferior jugular nodes. Function curves show change of accumulation count in lymph node of each region for 20 minutes.

used for evaluation of lymph node function: the right and left superior levels (ROI numbers 1 and 2), the mid levels (ROI numbers 3 and 4), and the inferior levels (ROI numbers 5 and 6) (Fig 1, *A*). The frame data obtained were used to generate "function curves" (Fig 1, *B*). These curves indicate the change in signal intensity as a function of the time elapsed, that is, the change in flow of the radioactive agent along the internal jugular chains. The curve numbers correspond to the ROI numbers.

Static lymphoscintigraphic images were obtained 3 hours after the injection with Tc-99m-Re and 30 minutes after the injection with Tc-99m-HSA-D. The patient was placed on a bed in a supine position under the scintillation camera. Static images were recorded on films.

When these 2 lymphoscintigraphies were performed, both injection areas were masked with a lead plate to inhibit the effect of the gamma-rays from those areas. The findings from the lymphoscintigraphy and palpation were compared with pathologic findings. The results were analyzed statistically (chi-square test) in regard to the diagnostic significance.

Palpation

Findings of lymph nodes by palpation were divided into 3 groups based on estimation of size: the size of the tip of a little finger or larger (L-size), smaller than the tip of a little finger (S-size), and nonpalpable (N-size). The size of the tip of a little finger was estimated to be 1.0 to 1.5 cm.

Pathologic examination

Surgically extirpated lymph nodes were examined pathologically and compared per level of neck nodes with lymphoscintigraphic and palpation findings.[15,16]

CASE REPORTS

Dynamic lymphoscintigraphy

Case 1: Fifty-year-old man with right mandibular carcinoma. This case showed an image pattern of inverse drainage between the right superior and mid internal jugular nodes (Fig 2, *A*).

Case 2: Sixty-three-year-old man with right lingual carcinoma. This case showed the image patterns of asymmetric drainage and delayed drainage between the right and left superior internal jugular nodes (Fig 2, *B*).

Static lymphoscintigraphy

Case 3: Fifty-one-year-old man with right lingual carcinoma. This case showed a defect in the right mid internal jugular node and a collateral pathway between the right superior and inferior jugular nodes (Fig 3, *A*).

Case 4: Thirty-six-year-old woman with right lingual carcinoma. This case showed a mottled-patchy pattern in the right mid internal jugular node and a swelling in the right superior jugular node (Fig 3, *B*).

Case 5: Sixty-five-year-old man with a carcinoma of the left oral floor. This case indicated a rope-like finding in the left mid and inferior jugular nodes and a swelling in the left superior jugular node (Fig 3, *C*).

RESULTS

Correlation of findings between pathologic examination, lymphoscintigraphy, and palpation was performed per level-to-level of neck lymph nodes of the superior, mid, and inferior internal jugular chains. The one-to-one contrast between individual lymph nodes was not done.

Correlation of pathologic specimens and the image patterns of defect, mottled-patchy, and swelling

To show the pathologic basis of lymphoscintigraphic image patterns, the 3 static lymphoscintigraphic image patterns of defect, mottled-patchy, and swelling were correlated to pathologic specimens when lymph nodes were surgically extirpated. The static lymphoscintigraphic results correlated closely with the pathologic findings (Fig 4). In the patterns of defect or mottled-patchy, the normal lymph node tissue disappeared entirely or was displaced by tumor in some degree. In

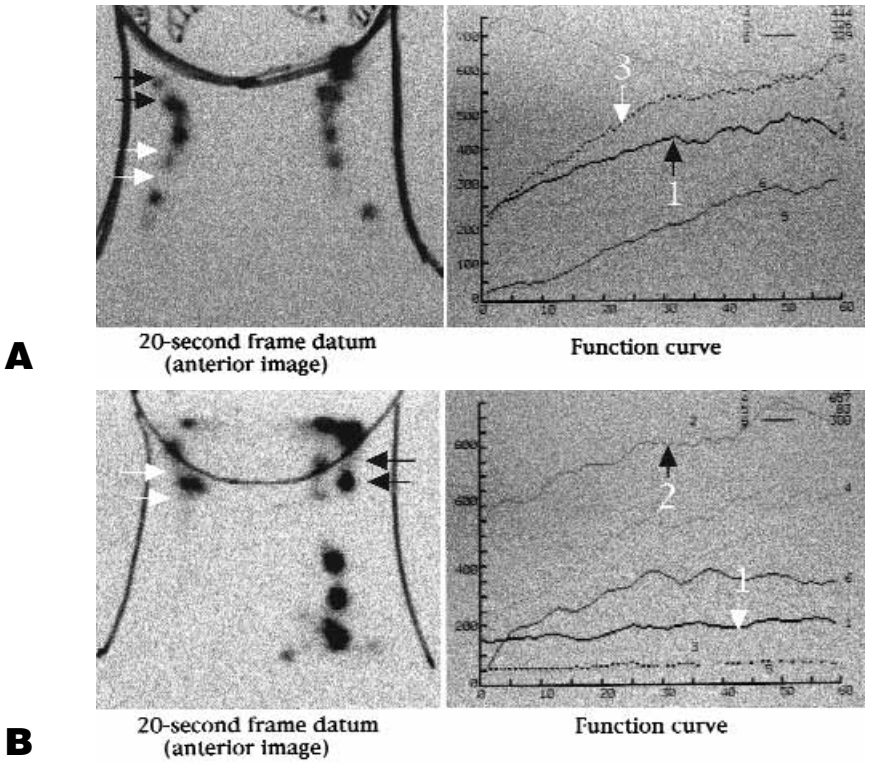

Fig 2. **A,** Case 1: Fifty-year-old man with right mandibular carcinoma. Radioactive count in right mid internal jugular node (curve No. 3, *white arrow*) exceeds that of right superior internal jugular node (curve No. 1, *black arrow*). This finding is interpreted to be an inverse drainage. **B,** Case 2: Sixty-three-year-old man with right lingual carcinoma. Lymphatic drainages in right and left internal jugular chains are very different and show asymmetric drainage. Radioactive count in right superior internal jugular node (curve No. 1, *white arrow*) is very low in comparison with left side (curve No. 2, *black arrow*). This finding is interpreted to be a delayed drainage of right superior internal jugular node.

Table II. Correlation between pathologic examination, dynamic lymphoscintigraphy with Tc-99m-Re, and palpation

Pathologic examination		*Dynamic lymphoscintigraphy*		*Palpation**		
				L-size	*S-size*	*N-size*
Metastatic	10 cases	Positive	10†	5	2	3
		Negative	0	0	0	0
Normal	7 cases	Positive	4‡	2	1	1
		Negative	3	0	1	2

*L-size indicates size of tip of little finger or larger; S-size, smaller than tip of a little finger; N-size, nonpalpable.
†Asymmetric drainage was shown in 10 cases, delayed drainage in 10, inverse drainage in 1.
‡Asymmetric drainage was shown in 4 cases, delayed drainage in 4, inverse drainage in 2.

the pattern of swelling, the lymph node showed a reactive hyperplasia.

Correlation between pathologic examination, lymphoscintigraphy and palpation among patients

Dynamic lymphoscintigraphy

Dynamic lymphoscintigraphy with Tc-99m-Re was performed in 26 of 65 cases, 17 of which were examined pathologically (Table II). Ten cases were proven to be metastatic, and 7 cases showed normal results. Positive lymphoscintigraphic image patterns were observed in 14 cases, and the negative finding was observed in 3 cases. Ten of 14 positive cases were proved to be metastatic (5 cases showed L-size node, 2 cases showed S-size node, and 3 cases showed N-size node in palpation), but 4 cases were normal pathologically (2 cases showed L-size node, 1 case showed S-

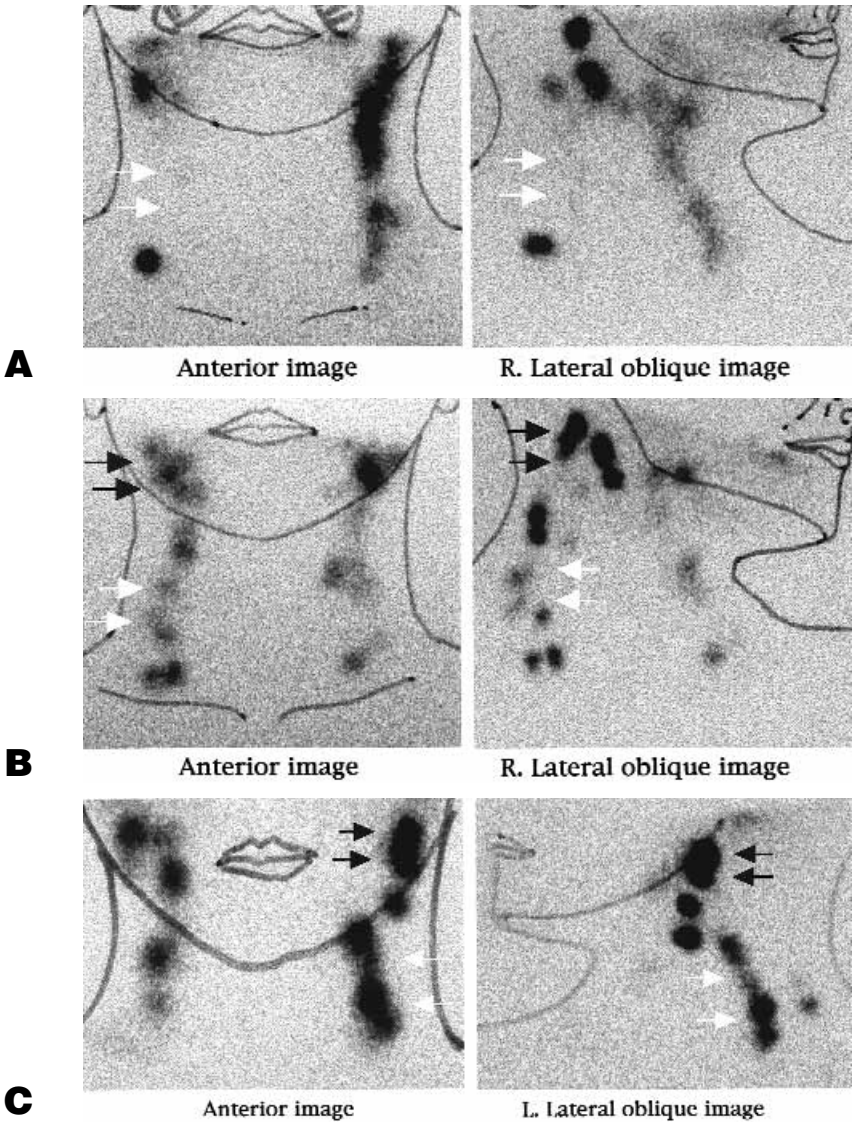

Fig 3. **A,** Case 3: Fifty-one-year-old man with right lingual carcinoma. Radioactive accumulation in right mid internal jugular node is not visible and shows defect *(white arrows)*. Right inferior internal jugular node shows almost normal radioactive accumulation in spite of defect in mid lymph node. This finding is interpreted to be a formation of a collateral pathway. **B,** Case 4: Thirty-six year-old woman with right lingual carcinoma. Radioactive accumulation in right mid internal jugular node decreases and image pattern of mottled-patchy is observed *(white arrows)*. Right superior internal jugular node shows increasing accumulation, and this image is interpreted to be a swelling *(black arrows)*. **C,** Case 5: Sixty-five-year-old man with carcinoma of left oral floor. Left mid and inferior internal jugular nodes increase radioactive accumulation. Isolation among individual lymph nodes is unclear, and it looks like a rope. This finding is interpreted to be a rope-like finding *(white arrows)*. Left superior internal jugular node shows image pattern of swelling *(black arrows)*.

size node, and 1 case showed N-size node). The 14 positive cases showed 3 lymphoscintigraphic image patterns: asymmetric drainage in 14 cases, delayed drainage in 14 cases, and inverse drainage in 3 cases. The 3 negative cases were normal in pathologic examination (1 case showed S-size node and 2 cases showed N-size node). On palpation, L-size node and S-size node (palpable) were observed in 11 cases, 7 cases of which were proven to be metastatic by pathologic examination. Six cases showed N-size lymph node (nonpalpable), but in half of them (3 cases), lymph nodes appeared to be metastatic pathologically. In dynamic lymphoscintigraphy with Tc-99m-Re, true-positive, true-negative, false-positive, and false-nega-

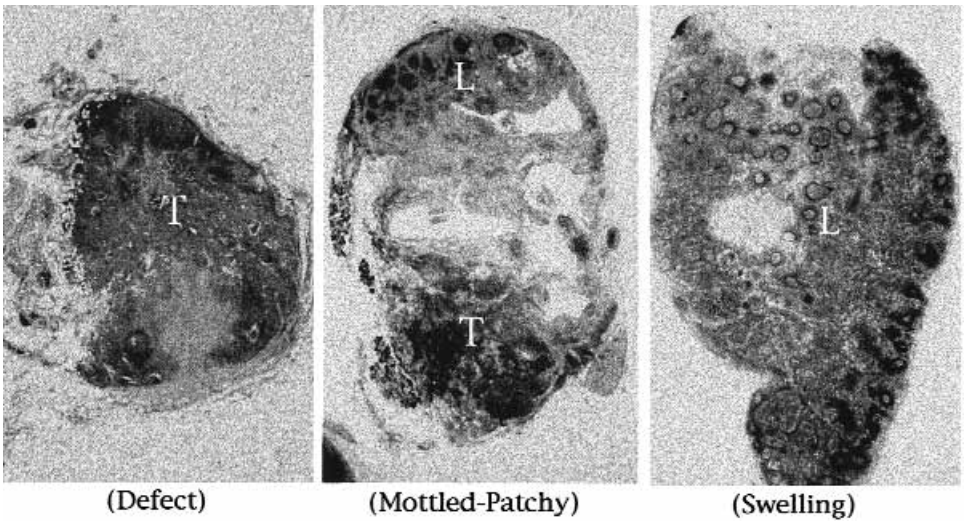

Fig 4. Three scintigraphic images of defect, mottled-patchy, and swelling are correlated with pathologic findings of surgically extirpated lymph nodes. In image pattern of defect, a majority of lymph node tissue is completely replaced by tumor *(T)*, and normal lymph node tissue is rarely observed. In image pattern of mottled-patchy, tumor tissue occupied half of lymph node tissue *(T)* but normal lymph node tissue is able to be observed *(L)*. In image pattern of swelling, most of lymph node tissue is kept in its normal condition *(L)*, and reactive hyperplasia of lymphatic follicles is observed.

Table III. Correlation between pathologic examination, dynamic lymphoscintigraphy with Tc-99m-HSA-D, and palpation

Pathologic examination		*Dynamic lymphoscintigraphy*		*Palpation**		
				L-size	*S-size*	*N-size*
Metastatic	9 cases	Positive	9†	2	3	4
		Negative	0	0	0	0
Normal	5 cases	Positive	5‡	0	0	5
		Negative	0	0	0	0

*L-size indicates size of tip of little finger or larger; S-size, smaller than tip of little finger; N-size, nonpalpable.
†Asymmetric drainage was shown in 9 cases, delayed drainage in 9, inverse drainage in 2.
‡Asymmetric drainage was shown in 5 cases, delayed drainage in 5.

tive were found in 10 of 14 cases (71%), 3 of 3 cases (100%), 4 of 14 cases (29%) and 0 of 3 cases (0%), respectively. Thus, the accuracy, sensitivity, and specificity were 76% (13/17), 100% (10/10), and 43% (3/7), respectively. On palpation, true-positive, true-negative, false-positive, and false-negative were observed in 7 of 11 cases (64%), 3 of 6 cases (50%), 4 of 11 cases (36%), and 3 of 6 cases (50%), respectively. The accuracy, sensitivity, and specificity were 59% (10/17), 70% (7/10), and 43% (3/7), respectively. The statistical analysis was done in regard to the diagnostic accuracy between dynamic lymphoscintigraphy with Tc-99m-Re and palpation, but no significant difference was observed (chi-square = 1.209 <2.706, $P = .10$).

Dynamic lymphoscintigraphy with Tc-99m-HSA-D was performed in 20 cases, of which 14 were examined pathologically (Table III). Nine cases were proven to be metastatic, and 5 cases showed normal results. Positive lymphoscintigraphic image patterns were observed in all 14 cases. Nine of 14 positive cases were proven to be metastatic (2 cases showed L-size node, 3 cases showed S-size node, and 4 cases showed N-size node), but 5 cases were normal pathologically (5 cases showed N-size node). The positive cases showed asymmetric drainage in 14 cases, delayed drainage in 14 cases, and inverse drainage in 2 cases. In palpation, L-size node and S-size node (palpable) were observed in 5 cases and proved to be metastatic by pathologic examination. Nine cases showed N-size node (nonpalpable), but in 4 cases, lymph nodes appeared to be metastatic pathologically. On dynamic lymphoscintigraphy with Tc-99m-HSA-D, true-positive, true-nega-

Table IV. Correlation between pathologic examination, static lymphoscintigraphy with Tc-99m-Re, and palpation

Pathologic examination		*Static lymphoscintigraphy*		*Palpation**		
				L-size	*S-size*	*N-size*
Metastatic	24 cases	Positive	24†	5	9	10
		Negative	0	0	0	0
Normal	8 cases	Positive	5‡	2	3	0
		Negative	3	0	0	3

*L-size indicates size of tip of little finger or larger; S-size, smaller than tip of little finger; N-size, nonpalpable.
†Defect was shown in 6 cases, mottled-patchy in 11 cases, swelling in 7 cases, collateral pathway in 2 cases, rope-like finding in 1 case.
‡Defect was shown in 4 cases, mottled-patchy in 1 case, swelling in 1 case, rope-like finding in 1 case.

tive, false-positive, and false-negative were found in 9 of 14 cases (64%), 0 cases, 5 of 14 cases (36%), and 0 cases, respectively. Thus, the accuracy, sensitivity, and specificity were 64% (9/14), 100% (9/9), and 0% (0/5), respectively. In palpation, true-positive, true-negative, false-positive, and false-negative were observed in 5 of 5 cases (100%), 5 of 9 cases (56%), 0 of 5 cases (0%), and 4 of 9 cases (44%), respectively. The accuracy, sensitivity, specificity were 71% (10/14), 56% (5/9), and 100% (5/5), respectively. The statistical analysis was done between dynamic lymphoscintigraphy with Tc-99m-HSA-D and palpation, but no significant difference was observed (chi-square = 0.1637 <2.706, $P = .10$).

Static lymphoscintigraphy

Static lymphoscintigraphy with Tc-99m-Re was performed in 65 cases, of which 32 were examined pathologically (Table IV). Twenty-four cases were proven to be metastatic, and 8 cases showed normal results. Positive lymphoscintigraphic image patterns were observed in 29 cases, and the negative finding was seen in 3 cases. Twenty-four of 29 positive cases were proven to be metastatic (5 cases showed L-size node, 9 cases showed S-size node, and 10 cases showed N-size node), but 5 cases were normal pathologically (2 cases showed L-size node and 3 cases showed S-size node). Twenty-nine positive cases showed 5 lymphoscintigraphic image patterns: defect in 20 cases, mottled-patchy in 12 cases, swelling in 8 cases, collateral pathway in 2 cases, and rope-like finding in 2 cases. Three negative cases were normal by pathologic examination (3 cases showed N-size node). On palpation, L-size node and S-size node (palpable) were observed in 19 cases, and 14 of them were proven to be metastatic by pathologic examination. Thirteen cases showed N-size node (nonpalpable), but in 10 of these cases, lymph nodes appeared to be metastatic pathologically. In static lymphoscintigraphy with Tc-99m-Re, true-positive, true-negative, false-positive, and false-negative were found in 24 of 29 cases (83%), 3 of 3 cases (100%), 5 of 29 cases (17%), and 0 of 3 cases (0%), respectively. Thus, the accuracy, sensitivity, and specificity were 84% (27/32), 100% (24/24), and 38% (3/8), respectively. In palpation, true-positive, true-negative, false-positive, and false-negative were observed in 14 of 19 cases (74%), 3 of 13 cases (23%), 5 of 19 cases (26%), and 10 of 13 cases (77%), respectively. The accuracy, sensitivity, and specificity were 53% (17/32), 58% (14/24), and 38% (3/8), respectively. The statistical analysis was done between static lymphoscintigraphy with Tc-99m-Re and palpation, and a significant difference was observed (chi-square = 7.272 >6.635, $P = .01$).

Static lymphoscintigraphy with Tc-99m-HSA-D was performed in 20 cases, of which 14 were examined pathologically (Table V). Nine cases were proven to be metastatic, and 5 cases showed normal results. Positive lymphoscintigraphic image patterns were observed in 13 cases, and 1 case showed a negative finding. Nine of 13 positive cases were proven to be metastatic (2 cases showed L-size node, 3 cases showed S-size node, and 4 cases showed N-size node), but 4 cases were normal pathologically (4 cases showed N-size node). These 13 positive cases showed 4 lymphoscintigraphic image patterns: defect in 6 cases, mottled-patchy in 3 cases, swelling in 8 cases, and collateral pathway in 3 cases. One negative case was proven to be normal pathologically (this case showed N-size node). On palpation, L-size node and S-size node (palpable) were observed in 5 cases and proven to be metastatic by pathologic examination. Nine cases showed N-size node (nonpalpable), but in 4 of these cases, lymph nodes appeared to be metastatic pathologically. In static lympho-scintigraphy with Tc-99m-HSA-D, true-positive, true-negative, false-positive, and false-negative were found in 9 of 13 cases (69%), 1 of 1 case (100%), 4 of 13 cases (31%), and 0 of 1 case (0%), respectively. The accuracy, sensitivity, and specificity were 71% (10/14), 100% (9/9), and 20% (1/5), respectively. On palpation, true-positive, true-negative, false-positive, and false-negative were observed in 5 of 5 cases (100%), 5 of 9 cases (56%), 0 of 5 cases (0%), and 4 of 9 cases (44%), respectively. The accuracy, sensitivity, specificity were 71% (10/14), 56% (5/9), and 100% (5/5), respectively. The statistical analysis was

Table V. Correlation between pathologic examination, static lymphoscintigraphy with Tc-99m-HSA-D, and palpation

Pathologic examination		*Static lymphoscintigraphy*		*Palpation**		
				L-size	*S-size*	*N-size*
Metastatic	9 cases	Positive	9†	2	3	4
		Negative	0	0	0	0
Normal	5 cases	Positive	4‡	0	0	4
		Negative	1	0	0	1

*L-size indicates size of tip of little finger or larger; S-size, smaller than tip of little finger; N-size, nonpalpable.
†Defect was shown in 5 cases, mottled-patchy in 2 cases, swelling in 5 cases, collateral pathway in 3 cases.
‡Defect was shown in 1 case, mottled-patchy in 1 case, swelling in 3 cases.

Table VI. Incidence of extra positive findings of static lymphoscintigraphy per level of neck lymph nodes

Level of metastatic lymph nodes (pathologic examination)	*Static lymphoscintigraphy (% of findings)*					
	Tc-99m-Re (24 cases)			*Tc-99m-HSA-D (9 cases)*		
	Superior	*Mid*	*Inferior*	*Superior*	*Mid*	*Inferior*
Superior	22	33	45	16	42	42
Mid	13	46	41	20	40	40
Inferior	18	35	47	20	40	40
Average of agreement		38%			32%	

done between static lymphoscintigraphy with Tc-99m-HSA-D and palpation, but no significant difference was observed (chi-square = 0 <2.706, $P = .10$).

Incidence of extra positive finding of static lymphoscintigraphy

A comparison per level of neck nodes between pathologic findings and static lymphoscintigraphy was performed in 24 cases with Tc-99m-Re and in 9 cases with Tc-99m-HSA-D (Table VI). All cases showed lymph node metastases pathologically in one or more levels of neck nodes, and static lymphoscintigraphy also showed positive findings in those levels of metastatic nodes. However, most of these cases showed one or more extra positive findings from static lymphoscintigraphy in some other levels of neck nodes that were normal pathologically. Incidence of extra positive finding of static lymphoscintigraphy per level of neck nodes is shown in Table VI. In the superior level of metastatic lymph nodes, the incidence of extra positive findings with Tc-99m-Re was 33% and 45% in the mid and inferior levels of neck nodes, respectively. In the mid level of metastatic lymph nodes, the incidence was 13% and 41% in the superior and inferior levels, and in the inferior level of metastatic lymph nodes, the incidences of 18% and 35% were observed in the superior and mid levels, respectively. The agreement was 22%, 46%, and 47% in the superior, mid, and inferior levels, respectively. The tendency of incidence of extra positive findings with Tc-99m-HSA-D was almost the same. The averages of agreement were 38% between pathologic examination and static lymphoscintigraphy with Tc-99m-Re and 32% with Tc-99m-HSA-D. The static lymphoscintigraphy tended to show 1 or more extra positive findings in the normal levels of neck nodes, and this tendency was slightly more distinct in Tc-99m-HSA-D. These results are thought to lead to the increase of false-positive or overestimation with lymphoscintigraphy.

Comparison between Tc-99m-Re, Tc-99m-HSA-D, and palpation

The accuracy, sensitivity, specificity, true-positive, true-negative, false-positive, and false-negative of lymphoscintigraphy and palpation are shown in Table VII. The results show that lymphoscintigraphy was superior to palpation in the accuracy, sensitivity, true-negative, and false-negative. However, lymphoscintigraphy showed a low specificity. Comparing Tc-99m-Re with Tc-99m-HSA-D, lymphoscintigraphy with Tc-99m-Re was estimated to be superior to that with Tc-99m-HSA-D in accuracy, specificity, true-positive, and false-positive. Statistical analysis showed a significant difference only between the static lymphoscintigraphy with Tc-99m-Re and palpation (chi-square = 7.272 >6.635, = .01). From the results, lymphoscintigraphy, especially the static lymphoscintigraphy with Tc-99m-Re, was proven to be superior to palpation to some degree.

Comparison between dynamic and static lymphoscintigraphy

Comparison of dynamic and static lymphoscintigraphy with Tc-99m-Re was performed on 17 patients, who were examined pathologically (Table VIII). Ten cases with metastasis showed 21 findings in dynamic and 23 findings in static lymphoscintigraphy in total. Seven cases without metastasis showed 10 findings in dynamic and 4 findings in static lymphoscintigraphy.

Table VII. Diagnostic reliability of Tc-99m-Re, Tc-99m-HSA-D, and palpation

		Statistical data (%)							
		Acc	*Sen*	*Spe*	*Tpos*	*Tneg*	*Fpos*	*Fneg*	*Chi-square*[*]
Tc-99m-Re	Dynamic (17 cases)	76	100	43	71	100	29	0	1.209
	Static (32 cases)	84	100	38	83	100	17	0	7.272
Tc-99m-HSA-D	Dynamic (14 cases)	64	100	0	64	–	36	–	0.1637
	Static (14 cases)	71	100	20	69	100	31	0	0
Palpation	(17 cases)	59	70	43	64	50	36	50	
	(32 cases)	53	58	38	74	23	26	77	
	(14 cases)	71	56	100	100	56	0	44	

Acc, Accuracy; *Sen,* sensitivity; *Spe,* specificity, *Tpos,* true-negative; *Fpos,* false-positive; *Fneg,* false-negative.
[*]Statistical significance.

Table VIII. Comparison between dynamic and static lymphoscintigraphy with Tc-99m-Re

	No. of cases in all			
Pathologic examination	*Dynamic*		*Static*	
Metastatic (10 cases)	Asymmetry	10	Defect	6
			Mottled-patchy	8
	Delayed	10 (21)	Swelling	6 (23)
			Collateral pathway	2
	Inverse	1	Rope-like finding	1
Normal (7 cases)	Asymmetry	4	Defect	2
			Mottled-patchy	1
	Delayed	4 (10)	Swelling	1 (4)
			Collateral pathway	0
	Inverse	2	Rope-like finding	0

Positive scintigraphic findings in accordance with pathologic examination were shown in 68% (21/31) of dynamic and 85% (23/27) of static lymphoscintigraphy. Comparison of dynamic and static lymphoscintigraphy with Tc-99m-HSA-D was performed on 14 patients, who were examined pathologically (Table IX). Nine cases with metastasis showed 2 findings in dynamic and 15 findings in static lymphoscintigraphy. Five cases without metastasis showed 10 findings in dynamic and 5 findings in static lymphoscintigraphy. Positive findings in accordance with pathologic examination were shown in 67% (20/30) of dynamic and 75% (15/20) of static lymphoscintigraphy. The number of findings were shown in total, but the accuracy was higher in static than dynamic lymphoscintigraphy with both Tc-99m-Re and Tc-99m-HSA-D.

Relationship of primary tumor sites with levels of metastatic lymph nodes and static lymphoscintigraphic findings

Pathologic examination was performed in 46 cases, of which 33 cases was proven to be metastatic. The distribution of metastatic lymph nodes per level is shown in Table X. There were 9 in the superior level, 29 in the mid level, and 13 in the inferior level. Static lymphoscintigraphy was carried out in 85 cases, and 77 of them showed positive lymphoscintigraphic findings. The number of positive lymphoscintigraphic findings per level is also shown in Table X. There were 10 in the superior level, 63 in the mid level, and 52 in the inferior level. Each tumor site showed almost the same tendency, and the mid level was the most commonly affected level. There was no relationship between tumor sites and affected levels.

DISCUSSION

Lymphoscintigraphy was first reported by Sherman and Ter-Pogossian[17] and Sage et al[18] by using the radioactive gold (Au-198) colloid. This colloid was suitable because of its small particle size, but the physical half-life of 2.7 days is long, and the radiation dose to patients from the beta radiation is rather high. Recently, Tc-99m was introduced as a tracer for lymphoscintigraphy because of its convenient physical characteristics,[19] for example, a short physical half-life and a low radiation dose. Since the introduction of Tc-99m, lymphoscintigraphy has been used in various regions of the body[19-21]: parasternal region, axillary-infraclavicular region, retroperitoneal region, and of course the oral region. In Japan, Tc-99m-sulfur colloid and Tc-99m-Sn colloid at first had been used for lymphoscintigraphy, but now 2 radioactive agents, Tc-99m-Re and Tc-99m-HSA-D, are used. In this study, these 2 radioactive agents were

Table IX. Comparison between dynamic and static lymphoscintigraphy with Tc-99m-HSA-D

	No. of cases in all			
Pathologic examination	*Dynamic*		*Static*	
Metastatic (9 cases)	Asymmetry	9	Defect	5
			Mottled-patchy	2
	Delayed	9 (20)	Swelling	5 (15)
			Collateral pathway	3
	Inverse	2	Rope-like finding	0
Normal (5 cases)	Asymmetry	5	Defect	1
			Mottled-patchy	1
	Delayed	5 (10)	Swelling	3 (5)
			Collateral pathway	0
	Inverse	0	Rope-like finding	0

applied to 65 cases (Tc-99m-Re) and 20 cases (Tc-99m-HSA-D) with malignant tumors of oral regions, and the usefulness was compared. These 2 agents are composed of different components. The mechanisms of uptake of Tc-99m-Re and Tc-99m-HSA-D differ, and because of this, lymphoscintigraphic image patterns also differ. The image patterns of the lymph nodes were more clearly visible with Tc-99m-Re than those with Tc-99m-HSA-D, and the static lymphoscintigraphy with Tc-99m-Re was found to be suitable for the evaluation of individual lymph nodes in this study. For either agent, about 30% of the injected volume is taken up by small lymphatic vessels.[22,23] Of course, the more radioactive agent that is injected, the more is taken up by small lymphatic vessels.[24] Both radioactive agents reach the lymph nodes within 30 minutes,[8,25] but the optimal times to obtain scintigraphic images after the injection are different. Images with Tc-99m-Re were taken about 2 hours after injection, and images with Tc-99m-HSA-D were taken 30 minutes after injection.[7,12] This difference results chiefly from the different speed of clearance of the agents.[8,12,13] We selected 2 areas behind the ears for the injection, and we injected subcutaneously. Ohtake et al[24] reported that radioactive agents injected intracutaneously were taken into the small lymphatic vessels easier than those injected subcutaneously. This difference resulted from the tissue pressure around the injection area. However, the intracutaneous injection usually results in intense pain. Thus, we chose to inject by means of the subcutaneous route. The injected areas we selected were very close to the internal jugular chains, but we were able to get good images by masking the injection areas with a lead plate when the images were taken. Anezyris et al[26] and Ege[22] reported that an injection volume under 0.5 mL (74-148 MBq) was suitable for good images of lymphoscintigraphy. We injected 0.25 mL (37 MBq) of Tc-99m-Re and 0.1 mL (74 MBq) of Tc-99m-HSA-D into each area, and we got suitable images for diagnosis.

We carried out 2 types of scintigraphies, dynamic and static. Static lymphoscintigraphy showed an overall higher agreement with pathologic examination than dynamic lymphoscintigraphy with both Tc-99m-Re and Tc-99m-HSA-D. Dynamic lymphoscintigraphies with Tc-99m-Re and Tc-99m-HSA-D indicated no clear statistical significance in comparison with palpation. In static lymphoscintigraphy, Tc-99m-HSA-D did not show any significant difference, but Tc-99m-Re showed a clearly statistical significance in comparison with palpation. Tc-99m-Re also could detect the small metastatic lymph nodes of 10 cases that were not detected by palpation (N-size nodes). Tc-99m-Re showed a slightly higher agreement than Tc-99m-HSA-D (38% vs 32%) in the evaluation of incidence of extra positive findings. The lymphoscintigraphy showed an overall superiority in the accuracy, sensitivity, true-negative, and false-negative in comparison with palpation, though the statistical significance was only shown in the static lymphoscintigraphy with Tc-99m-Re. Sako et al[27] and Ali et al[28] reported almost the same results of palpation; that is, that the accuracy and false-negative were about 70% to 80% and 20% to 40%, respectively. From these results, we concluded that lymphoscintigraphy was superior to palpation, and Tc-99m-Re was more useful than Tc-99m-HSA-D as an agent for lymphoscintigraphy.

Nodal metastases in patients with oral malignant tumor were often observed in the levels of mid and inferior nodes in this study. Som[29] reported the same result; therefore, much attention has to be paid to those levels of neck nodes.

We also evaluated the significance of lymphoscintigraphy in comparison with CT, MRI, and US by a review of the literature. The modalities of CT, MRI, and US are frequently used for the purpose of detecting metastatic lymph nodes, and they are currently more common than lymphoscintigraphy. In some reports of CT, the sensitivity was reported to be 84%[5] or 60%,[30] specificity was 71%[5] or 99%,[30] and accuracy was 90%,[31] 93%,[32] or 85%.[30] In the reports of MRI, the

Table X. Relationship of primary tumor sites with levels of metastatic lymph nodes and static lymphoscintigraphic findings

	Level of metastatic lymph nodes (33 cases)			*Static lymphoscintigraphy (77 cases)*		
Primary tumor site	*Superior*	*Mid*	*Inferior*	*Superior*	*Mid*	*Inferior*
Maxilla	1	5	3	4	11	8
Buccal mucosa	1	1	0	1	3	3
Mandible	0	1	0	0	5	2
Tongue	2	6	2	0	19	18
Oral floor	0	8	2	2	16	12
Cervical region	5	8	6	3	9	9
Total	9	29	13	10	63	52

sensitivity was 92%[5] or 36%,[33] and specificity was 83%[5] or 94%.[33] The results of CT and MRI were superior to those of lymphoscintigraphy obtained in this study except for sensitivity. In the reports of US, the sensitivity was 91%[34] or 100%,[35] specificity was 56%[34] or 29%,[35] and accuracy was 81%[34] or 73%[35]; these results were similar to those of lymphoscintigraphy. These 3 types of modalities put their diagnostic criteria on the morphologic changes of lymph nodes, especially on the size of lymph nodes. Generally, size 1.0 to 1.5 cm is used as a cutoff point to determine malignancy, and this is an effective size criterion.[36,37] There is no doubt that most metastatic neck nodes are larger than normal nodes. However, some reports throw doubt on the size criterion of 1.0 to 1.5 cm because there is a large size-range overlap between normal and malignant lymph nodes. In the lymph nodes of borderline sizes 1.0 to 1.5 cm and 1.6 to 2.0 cm, the metastatic lymph nodes were found only in 16% and 29% of total nodes, respectively.[37] Even lymph nodes smaller than 1.0 cm often showed micrometastases and occult metastases.[38-41] Moreover, one report stated that nodal size bore a less direct relationship with metastases.[39] Thus, there is some doubt that the nodal size should be used as a diagnostic criterion by itself. The finding of central necrosis has been taken as an additional criterion to assist the size criterion. In fact, central necrosis larger than 3 mm was able to be detected with soft tissue resolution capabilities of most new-generation imaging modalities of CT or MRI[37,41] and was a highly reliable indicator of malignancy.[39] However, because the central necrosis depends on tumor progression at an early stage of the metastatic process, it is a rare phenomenon and will therefore not assist the nodal size in detecting metastatic nodes.[41]

On the other hand, lymphoscintigraphy uses a different diagnostic criterion from CT, MRI, and US, and lymphoscintigraphy puts its diagnostic criterion on the changes of lymph node function. Lymphoscintigraphy, of course, has some disadvantages as a modality for detecting lymph node metastases,[15,19,22,42-47] for example, in detecting the anatomic differences between individuals in the number of lymph nodes and in the distribution of lymph nodes per side and level. The injected nuclear agent is not taken equally in every lymph node. Moreover, this modality shows a high incidence of false-positive (overestimation) and low specificity.[43,44] This overestimation is, in fact, an undesirable phenomenon. This is assumed to be caused partly by the obstruction of small lymphatic vessels by tumor. When the lymphatic drainage is stopped or stagnated in the lymphatic vessels or lymph nodes of upper level, radioactive agents cannot reach the lymph nodes of the lower level. The obstruction leads to the defect image pattern (false-positive or overestimation) of normal lymph nodes in the lower level. This overestimation is assumed to be caused partly by the response of lymph nodes to inflammatory lesions because there are many odontogenic lesions in the oral region. These lymph nodes often show an image–pattern-like swelling in static lymphoscintigraphy. However, in spite of these disadvantages, this modality has many advantages,[6,16,48-53] for example, the high sensitivity and low incidence of false-negative. This method can display all levels of neck lymph nodes at one time and, importantly, this method can detect the functional changes in lymphatic systems. Moreover, this method could detect small metastatic lymph nodes (N-size node) in this study.

Although CT and MRI are actually very good modalities for detecting lymph node metastases, there are some problems with these modalities. Neither CT nor MRI could detect most of micrometastases,[38,39] and 10% to 15% of metastatic lymph nodes were estimated to be normal (false=negative) with CT or MRI.[54,55] There is also doubt on the size criterion. Thus, it is impossible to detect lymph node metastases completely by CT or MRI alone, and CT or MRI should be combined with some other modalities.[5,39,55] Lymphoscintigraphy is thought to be eligible to be combined with CT or MRI and will accomplish the role as a partner because lymphoscintigraphy uses a different

diagnostic criterion, detects the changes in lymphatic drainage and lymph node function, shows a very low incidence of false-negative, shows a very high sensitivity, displays all levels of neck lymph nodes at one time, and may be able to detect small lymph node metastases (N-size node). Therefore, lymphoscintigraphy should be performed before CT or MRI, making use of its superior characteristics. The levels of neck nodes that are suspected to be metastases by lymphoscintigraphy should be examined in detail by CT or MRI to decrease the incidence of false-positive and false-negative.[56] When the accuracy increases by a combination of CT or MRI with lymphoscintigraphy, the results will lead to the decrease of unnecessary elective neck treatment.

Recently, some new modalities have been assessed, for example, MRI with a new contrast agent,[57,58] the combination of Tl-201 single photon emission computed tomography with MRI,[59] positron emission tomography,[33,60-62] lymphoscintigraphy with double radioactive tracers,[63] and ultrasound-guided fine needle aspiration biopsy,[6,64-66] because 25% of all clinically occult lymph node metastases are too small to be detected by any currently available technique.[38] New modalities show a high diagnostic reliability, and these new modalities are expected to be generalized soon.

In summary, lymphoscintigraphy is superior to palpation in detecting metastases and has some important advantages that CT and MRI lack. This modality of lymphoscintigraphy can assist other imaging modalities as a preliminary technique for the evaluation of metastatic lymph nodes, making use of its superior characteristics.

We thank Mr Miguel Federico Vazquez Archdale for reading the manuscript.

REFERENCES

1. Anzai Y, Brunberg JA, Lufkin RB. Imaging of nodal metastases in the head and neck. J Magn Reson Imaging 1999;7:774-83.
2. Ege GN, Gummings BJ. Interstitial radiocolloid iliopelvic lymphoscintigraphy: technique, anatomy and clinical application. Int J Rad Oncol Biol Phys 1980;6:1483-90.
3. Blakeslee DB, Becker GD, Simpson GT, Pattern DH, Sprengelmeyer J. Lymphoscintigraphy of the neck. Otolaryngol Head Neck Surg 1985;93:361-5.
4. Bellin MF, Roy C, Kinkel K, Thoumas D, Zaim S, Vanel D, et al. Lymph node metastases: safety and effectiveness of MR imaging with ultrasmall super paramagnetic iron oxide particles—initial clinical experience. Radiology 1998;207:799-808.
5. Hillsamer PJ, Schuller DE, McGhee RB, Chakeres D, Young DC. Improving diagnostic accuracy of cervical metastases with computed tomography and magnetic resonance imaging. Arch Otolaryngol Head Neck Surg 1990;116:1297-1301.
6. De Jong RJB, Rongen RJ, Verwoerd CDA, Van Overhangen H, Lameris JS, Knegt P. Ultrasound-guided fine-needle aspiration biopsy of neck nodes. Arch Otolaryngol Head Neck Surg 1991;117:402-4.
7. Sato T, Morita Y, Kawano K, Suenaga S, Tomomura A, Noikura T. Clinical evaluation of lymphoscintigraphy of the head and neck. Oral Radiol 1989;5:1-9.
8. Nagai K, Ito Y, Otsuka N, Muranaka A, Kaji T, Terashima H, et al. Clinical usefulness on accumulation of 99m-Tc rhenium colloid in lymph nodes (Japanese). Radioisotopes 1980;29:549-51.
9. Pecking A, Le Mercier N, Gobin R, Bardy A, Najean Y. Résultatés préliminaries de l'éssai du un nouveau composé pour lymphographies isotopiques: le sulfure de rhénium colloidal marqué par du technétium-99m. J Fr Biophys Et Med Nucl 1978;2:117-20.
10. Strand SE, Person BRR. Quantitative lymphoscintigraphy I: basic concepts for optimal uptake of radiocolloids in the parasternal lymph nodes of rabbits. J Nucl Med 1979;20:1038-46.
11. Takahashi T, Kikuchi M, Obara T, Yanagisawa T. Lymphoscintigraphy with 99m-Tc-DTPA-HSA: detection of metastasis to lymphatic system (Japanese). Radioisotopes 1992;41:439-43.
12. Ohtake E, Matsui K, Kobayashi Y, Ono Y. Dynamic lymphoscintigraphy with Tc-99m human serum albumin. Radiation Med 1983;1:132-6.
13. Kikuchi M, Takahashi T, Kato K, Oikawa H, Obara T, Yanagisawa T, et al. Lymphoscintigraphy with 99m-Tc-DTPA-HSA in the diagnosis of protein-losing gastroenteropathy (Japanese). Jpn J Nucl Med 1993;30:203-7.
14. Henze E, Schelbert HR, Collins JD, Najafi A, Barrio JR, Bennett LR. Lymphoscintigraphy with Tc-99m-labeled dextran. J Nucl Med 1982;23:923-9.
15. Glassburn JR, Prasasvinichia S, Nuss RC, Croll MN, Brady LW. Correlation of Au-198 abdominal lymph scans with lymphangiograms and lymph node biopsies. Radiology 1972;105:93-6.
16. Kazem I, Antoniades J, Brady LW, Faust DS, Croll MN, Lightfoot D. Clinical evaluation of lymph node scanning utilizing colloidal gold 198. Radiology 1968;90:905-11.
17. Sherman AI, Ter-Pogossian M. Lymph node concentration of radioactive colloidal gold following interstitial injection. Cancer 1953;6:1238-90.
18. Sage HH, Kizilay D, Miyazaki M, Shapiro G, Sinha B. Lymph node scintigrams. Am J Roentgenol 1960;84:666-72.
19. Fairbanks VF, Tauxe WN, Kiely JM, Miller We. Scientific visualization of abdominal lymph nodes with 99m-Tc-pertechnetate-labeled sulfur colloid. J Nucl Med 1971;13:185-90.
20. Frank V, Charles MB. Radionuclide lymphangiography in evaluation of pediatric patients with lower-extremity edema: concise communication. J Nucl Med 1977;18:441-4.
21. Hauser W, Atkins HL, Richards P. Lymph node scanning with 99m-Tc-sulfur colloid. Radiology 1969;92:1369-71.
22. Ege GN. Internal mammary lymphoscintigraphy. The rationale, technique, interpretation and clinical application: a review based on 848 cases. Radiology 1976;118:101-7.
23. Alavi A, Staum MM, Shesol BF, Bloch PH. Technetium-99m stannous phytate as an imaging agent for lymph nodes. J Nucl Med 1978;19:422-6.
24. Ohtake E, Matsui K, Lymphoscintigraphy in patients with lymphedema. A new approach using intradermal injections of technitium-99m human serum albumin. Clin Nucl Med 1986;11:474-8.
25. McNeill GC, Witte MH, Witte CL, Williams WH, Hall JN, Patton DD, et al. Whole-body lymphangioscintigraphy: preferred method for initial assessment of the peripheral lymphatic system. Radiology 1989;172:495-502.
26. Anezyris N, Sawas-Dimopoulou C, Dontas N, Samaras SE. Thoracic lymph node scintiscan as a diagnostic test in mediastinal malignant enlargement. Chest 1971;59:372-7.
27. Sako K, Pradier RN, Marchetta FC, Pickren JW. Fallibility of palpation in the diagnosis of metastases to cervical nodes. Surg Gynecol Obstet 1964;118:989-90.
28. Ali S, Tiwari RM, Snow GB. False-positive and false-negative neck nodes. Head Neck Surg 1985;8:78-82.
29. Som PM. Lymph nodes of the neck. Radiology 1987;165:593-600.
30. Watanabe K, Noikura T, Yamashita S, Fukunaga M, Orita K, Nakano S, et al. Phase III trial of Tc-99m-Rhenium colloid for lymphoscintigraphy (Japanese). Jpn J Nucl Med 1992;29:979-90.
31. Friedman M, Shelton VK, Mafee M, Bellity P, Grybauskas V, Skolnik E. Metastatic neck disease—evaluation by computed tomography. Arch Otolaryngol 1984;110:443-7.

32. Stevens MH, Harnsberger HR, Mancuso AA, Davis RK, Johnson LP, Parkin JL. Computed tomography of cervical lymph nodes—staging and management of head and neck cancer. Arch Otolaryngol 1985;111:735-9.
33. Braams JW, Pruim P, Freling NJM, Nikkels PGJ, Roodenburg JLN, Boering G, et al. Detection of lymph node metastases of squamous-cell cancer of the head and neck with FDG-PET and MRI. J Nucl Med 1995;36:211-6.
34. Ohta M. The trial of ultrasonography for metastatic lymph nodes and investigation of radiotherapeutic effect with ultrasonography (Japanese). J Kurume Med Assoc 1986;49:17-28.
35. Yamaguchi K. Diagnostic studies on the regional lymph node metastases of oral squamous cell carcinoma—evaluation of lymph node metastases utilizing ultrasound sonography and lymphoscintigraphy (Japanese). Jpn J Oral Maxillofac Surg 1991;37:1571-91.
36. Friedman M, Roberts N, Kirshenbaum GL, Colombo J. Nodal size of metastatic squamous cell carcinoma of neck. Laryngoscope 1993;103:854-6.
37. Van den Brekel MWM, Stel HV, Castelijns JA, Nauta JJP, Van der Waal I, Valk J, et al. Cervical lymph node metastasis: assessment of radiologic criteria. Radiology 1990;177:379-84.
38. Van den Brekel MWM, Van der Waal I, Meijer CJLM, Freeman JL, Castelijns JA, Snow GB. The incidence of micrometastases in neck dissection specimens obtained from elective neck dissections. Laryngoscope 1996;106:987-91.
39. Stern WBR, Silver CE, Zeifer BA, Persky MS, Heller KS. Computed tomography of the clinically negative neck. Head Neck 1990;12:109-13.
40. Don DM, Anzai Y, Lufkin RB, Fu YS, Calcaterra TC. Evaluation of cervical lymph node metastases in squamous cell carcinoma of the head and neck. Laryngoscope 1995;105:669-74.
41. Feimesser R, Freeman JL, Feinmesser M, Noyek A, Mullen JBM. Role of modern imaging in decision-making for elective neck dissection. Head Neck 1992;14:173-6.
42. Zum Winkel K, Hermann HJ. Scintigraphy of lymph nodes. Lymphology 1977;10:107-14.
43. Seaman WB, Powers WE. Studies on the distribution of radioactive colloidal gold in regional lymph nodes containing cancer. Cancer 1955;8:1044-6.
44. Matsuo S. Studies on the metastasis of breast cancer to lymph nodes. II. Diagnosis of metastasis to internal mammary nodes using radiocolloid (Japanese). Acta Med Okayama 1975;28:361-371.
45. Thommesen P, Buhl J, Jansen K, Funch-Jensen P. Lymphoscintigraphy in the head and neck in normals diagnostic value. Fortschr Rontgenstr 1981;134:80-2.
46. Aspegren K, Strand SE, Persson BRR. Quantitative lymphoscintigraphy for detection of metastases to the internal mammary lymph nodes. Biokinetics of 99m-Tc sulphur colloid uptake and correlation with microscopy. Acta Radiol (Oncology) 1978;17:17-26.
47. Pearlman AW. Abdominal lymph node lymphoscintigraphy with radioactive gold (198-Au) for evaluation and treatment of patients with lymphoma. Am J Roentgenol 1970;109:780-92.
48. Gates GF, Dore EK. Primary congenital lymphedema in infancy evaluated by isotope lymphangiography. J Nucl Med 1971;12:315-7.
49. Rees WV, Robinson DS, Holmes EC, Morton DL. Altered lymphatic drainage following lymphadenoectomy. Cancer 1980;45:3045-9.
50. Terui S, Kato H, Hirashima T, Iizuka T, Oyamada H. An evaluation of the mediastinal lymphoscintigram for carcinoma of the esophagus studied with 99m-Tc rhenium sulfur colloid. Eur J Nucl Med 1982;7:99-101.
51. Gabelle PH, Comet M, Bodin JP, Dupre A, Carpentier E, Bolla M, et al. La lymphoscintigraphie mammaire par injection intratumorale dans le bilan du cancer du sei. Nouv Press Med 1981;10:3067-70.
52. Salvatore M, Avitabile G, Muto V. Scintigraphy in the problem of metastases from cancer of the larynx. Revue de Laryngologie 1981;102:535-41.
53. Vaqueiro M, Gloviczki P, Fisher J, Hollier LH, Schirger A, Wahner HW. Lymphoscintigraphy in lymphedema: an aid to microsurgery. J Nucl Med 1986;27:1125-30.
54. Friedman M, Mafee MF, Pacella BL, Strorigl TL, Dew LL, Toriumi M. Rationale for elective neck dissection in 1990. Laryngoscope 1990;100:54-9.
55. Van den Brekel MWM, Castelijns JA, Croll GA, Stel HV, Valk J, Van der Waal I, et al. Magnetic resonance imaging vs palpation of cervical lymph node metastasis. Arch Otolaryngol Head Neck Surg 1991;117:666-73.
56. Watanabe K, Hoshi H, Nakayama S, Yasumori K. Clinical significance of lymphoscintigraphy: a review (Japanese). Jpn J Clin Radiol 1981;26:1361-9.
57. Anzai Y, Blackwell KE, Hirschowitz SL, Rogers JW, Sato Y, Yuh WTC, et al. Initial clinical experience with dextran-coated superparamagnetic iron oxide for detection of lymph node metastases in patients with head and neck cancer. Radiology 1994;192:709-15.
58. Weissleder R, Elizondo G, Wittenberg J, Lee AS, Josephson L, Brady TJ. Ultrasmall superparamagnetic iron oxide: an intravenous contrast agent for assessing lymph nodes with MR imaging. Radiology 1990;175:494-8.
59. Olmos RAV, Koops W, Loftus BM, Liem IH, Gregor RT, Hoefnagel CA, et al. Correlative Tl-201 SPECT, MRI and ex vivo Tl-201 uptake in detecting and characterizing cervical lymphadenopathy in head and neck squamous cell carcinoma. J Nucl Med 1999;40:1414-9.
60. Anzai Y, Minoshima S, Wolf GT, Wahl RL. Head and neck cancer: detection of recurrence with three-dimensional principal components analysis at dynamic FDG PET. Radiology 1999;212:285-90.
61. Aassar OS, Fischbein NJ, Caputo GR, Kaplan MJ, Price DC, Singer MI, et al. Metastatic head and neck cancer: role and usefulness of FDG PET in locating occult primary tumors. Radiology 1999;210:177-81.
62. Laubenbacher C, Saumweber D, Manslau CW, Kau RJ, Herz M, Avril N, et al. Comparison of fluorine-18-fluorodeoxyglucose PET, MRI and endoscopy for staging head and neck squamous-cell carcinomas. J Nucl Med 1995;36:1747-57.
63. Klutmann S, Bohuslavizki KH, Brenner W, Hoft S, Kroger S, Werner JA, et al. Lymphoscintigraphy in tumors of the head and neck using double tracer technique. J Nucl Med 1999;40:776-82.
64. Schwarz R, Chan NH, MacFarlane JK. Fine needle aspiration cytology in the evaluation of head and neck masses. Am J Surg 1990;159:482-5.
65. Baatenburg de Jong RJ, Knegt P, Verwoerd CDA. Reduction of the number of neck treatments in patients with head and neck cancer. Cancer 1993;71:2312-8.
66. Takes RP, Knegt P, Manni JJ, Meeuwis CA, Marres HM, Spoelstra HAA, et al. Regional metastasis in head and neck squamous cell carcinoma: revised value of US with US-guided FNAB. Radiology 1996;198:819-23.

Reprint requests:

Tsuyoshi Sato, DDS
Department of Dental Radiology
Kagoshima University Dental School
8-35-1 Sakuragaoka
Kagoshima 890-8544, Japan
sato@denta.hal.kagoshima-u.ac.jp